Intraoperative Infrared Functional Imaging of Human Brain

Alexander M. Gorbach, PhD,[1,2] John Heiss, MD,[1] Conrad Kufta, MD,[1] Susumo Sato, MD,[3] Paul Fedio, PhD,[4] William A. Kammerer, MD,[5] Jeffrey Solomon, MS,[6] and Edward H. Oldfield, MD[1]

We hypothesized that it would be possible to detect the distribution of cortical activation by using a sensitive, rapid, high-resolution infrared imaging technique to monitor changes in local cerebral blood flow induced by changes in focal cortical metabolism. In a prospective study, we recorded in 21 patients the emission of infrared radiation from the exposed human cerebral cortex at baseline, during language and motor tasks, and during stimulation of the contralateral median nerve using an infrared camera (sensitivity 0.02°C). The language and sensorimotor cortex was identified by standard mapping methods (cortical stimulation, median nerve somatosensory-evoked potential, functional magnetic resonance imaging), which were compared with infrared functional localization. The temperature gradients measured during surgery are dominated by changes in local cerebral blood flow associated with evoked functional activation. The distribution of the evoked temperature changes overlaps with, but extends beyond, functional regions identified by standard mapping techniques. The distribution observed via infrared mapping is consistent with distributed and complex functional representation of the cerebral cortex, rather than the traditional concept of discrete functional loci demonstrated by brief cortical stimulation during surgery and by noninvasive functional imaging techniques. By providing information on the spatial and temporal patterns of sensory-motor and language representation, infrared imaging may prove to be a useful approach to study brain function.

Ann Neurol 2003;54:297–309

Although usually presented as a measure of neuronal activity, functional imaging techniques, including positron emission tomography, functional magnetic resonance imaging (fMRI), and optical intrinsic imaging, measure either the rate of consumption of an energy substrate (glucose, oxygen) or neurophysiological responses to such consumption (rate of local cerebral blood flow [CBF]). Cortical regions of increased functional activity also are identified by energy released in the form of electrogenesis (action potentials) or intrinsic production of heat. Correlation of the timing and localization of heat production of brain structures to functional activation has been previously examined.[1] Thermocouples have been used to measure stimulation-induced temperature shifts during presentation of visual, somesthetic, and auditory stimuli.[2–4] However, thermocouples compress adjacent vessels, modifying CBF-dependent local heat dissipation, and the studies are inconclusive for location of temperature foci, its spatial heterogeneity, and location of function. Gorbach mapped stimulation-induced temperature responses in the brain using infrared imaging through the animal scalp and correlated stimulation of rat whiskers with localization of the cortical temperature responses.[5,6] However, these experiments did not determine if the detected shifts in brain temperature were a result of changes in neuronal metabolism or cerebral blood flow.

We hypothesized that evaporation from the exposed brain would increase the rate of heat dissipation, enhancing discrimination of local thermal gradients and the capacity to localize cortical activity by neuronal heat production or by the increased capillary blood flow that is tightly linked regionally and temporally to increased neural firing.[7,8] Success would allow precise imaging of cortical functional activation in time and space.

From the [1]Surgical Neurology Branch, National Institute of Neurological Disorders and Stroke; [2]Department of Radiology, Warren Grant Magnuson Clinical Center; [3]Office of Clinical Director, National Institute of Neurological Disorders and Stroke, National Institutes of Health, Bethesda, MD; [4]Department of Psychology, George Mason University, Fairfax, VA; [5]Department of Anesthesiology, Warren Grant Magnuson Clinical Center, National Institutes of Health, Bethesda, MD; and [6]Sensor Systems Inc., Sterling, VA.

Received Nov 25, 2002, and in revised form Feb 25 and Apr 11, 2003. Accepted for publication Apr 11, 2003.

Address correspondence to Dr Oldfield, National Institutes of Health, NINDS, Surgical Neurology Branch, Building 10, Room 5D37, Bethesda, MD 20892. E-mail: eo10d@nih.gov

Materials and Methods

Patients

Twenty-one adults (8 women, 13 men, aged 21–68 years) whose surgery would expose cortical regions amenable to intraoperative functional mapping were eligible for this prospective study (protocol 96-N-0093). The need for surgery was established independently using conventional clinical indications. Local anesthesia with intravenous sedation (fentanyl, midazolam, and propofol) was chosen for 16 patients undergoing intraoperative speech mapping, somatosensory-evoked potential (SSEP) mapping, and infrared (IR) imaging. Five patients received surgery under general anesthesia, and SSEP mapping and IR imaging were performed. General anesthesia was induced with propofol; maintenance anesthesia included fentanyl, cisatracurium, oxygen, nitrous oxide, and isoflurane. Isoflurane was discontinued before testing. Twenty patients had brain tumors and one had had medically intractable epilepsy (Table).

Infrared Imaging

An advanced digital IR camera (Infrared Focal Plane Array camera, Lockheed Martin IR Imaging Systems, Goleta, CA) was used to image local temperature gradients across the cerebral cortex by passively detecting IR emission. As IR emission at the measured wavelength (3–5μm) is directly proportional to temperature, the camera was calibrated in units of temperature. It has a sensitivity of 0.02°C. One hundred images (256 × 256 pixels) were obtained at intervals of 14 to 600 milliseconds and digitized at 14 bits per pixel. The camera was placed 10 to 30cm above the exposed brain surface to achieve a field of view that fit the area of the cortex exposed (35 × 35mm to 100 × 100mm), producing spatial resolution for individual pixels of 100 × 100μm to 350 × 350μm.

The camera was attached to a ceiling mount for an operating room light and covered with sterile draping. After cooling the camera detector and loading a previously stored two-point temperature calibration file into the computer, the camera was ready. With the camera positioned with the plane of the lens parallel to the plane of the exposed brain sequential, digital images were taken. Automated image acquisition started at the same point in the respiratory and cardiac cycles to reduce the effects of physiological motion.

Background IR imaging (two to three trials per patient)

Table. Correlation of Infrared Results with Standard Methods of Cortical Localization

Patient No.	Age (yr)/ Sex	Side	Location	Anesthesia	Pathology	Comparison of Infrared with Standard Methods			
						Sensory Cortex		Motor Cortex Stimulation	Language Stimulation
						SSEP	Stimulation		
1	50/F	R	Inferior frontal	Local	Oligodendroglioma	B B B	B C B		
2	21/F	L	Temporal	Local	Oligodendroglioma	B A A	B A A		B
3	50/M	R	Frontal	General	Glioblastoma multiforme	A B B	B B B		
4	58/M	L	Parasagittal frontal	Local	Oligodendroglioma/astrocytoma	B A A	A B B	B B B	
5	68/M	R	Frontoparietal	Local	Glioblastoma multiforme	A B A	B A B	B B B	
6	48/M	R	Temporoparietal	General	Oligodendroglioma/astrocytoma	B B B	A B B		
7	30/M	L	Parietal	Local	Anaplastic oligodendroglioma	A C B	A B A	A C B	
8	35/M	R	Temporoparietal	Local	Glioblastoma multiforme			B B B	
9	55/F	R	Frontoparietal	Local	Glioblastoma	B A B	B B B	C B B	
10	27/M	L	Frontal	Local	Anaplastic astrocytoma	B A B	C B B	B C B	B
11	63/M	R	Parietal	Local	Astrocytosis/radiation necrosis	B C B[a]	C B C	B B B	
12	39/F	R	Parietal	Local	Metastatic melanoma	C B B[a]	C A B	A B B	
13	30/M	L	Temporal	Local	Anaplastic oligodendroglioma	A A A	B A A	B B B	C
14	24/F	L	Temporal	Local	Oligodendroglioma			A B A	B
15	47/M	L	Temporoparietal	General	Oligodendroglioma	A B A	B B B		
16	68/M	L	Temporal	Local	Glioblastoma				B
17	29/M	L	Frontal	Local	Glioblastoma	C A B[b]	B C C		
18	48/F	R	Frontalparietal	Local	Metastatic colonic adenocarcinoma	B B B	B A B	A B B	
19	40/M	L	Frontotemporal	General	Medically intractable epilepsy	B A A	A B B		
20	30/F	R	Parietalfrontal lobe	Local	Giant cell glioblastoma	A B B	B B B		
21	43/F	L	Frontoparietal	General	Falx meningioma	A B A	C A B		

[a]Only sensory cortex.
[b]Only motor cortex was identified with SSEP.

A = IR focus within; B = IR focus partially inside; C = IR focus outside the circle indicated by standard localization; SSEP = somatosensory-evoked potentials; R = right; L = left.

was performed by acquisition of spontaneous IR emission for 1 minute. Imaging was repeated during functional tasks (patients receiving local anesthesia) and during median nerve stimulation (local and general anesthesia); three trials were performed for sensory and motor functional tests and one trial for the language tests (1.5–2.0 minutes intertrial duration). The motor tasks (11 patients) were finger tapping and serially squeezing a ball, initiated 12 to 16 seconds after beginning acquisition of IR images (data acquisition, 36.4 seconds) and continued for 10 to 15 seconds at 1 to 4 per second. Contralateral median nerve stimulation (model S8800; Grass Instrument, W. Warwick, RI) was initiated after beginning acquisition of IR images (acquisition time, 1.4–15.4 seconds) using standard parameters (0.3 milliseconds monophasic pulses at 4Hz; 3–10mA). Verbal tasks (six patients) consisting of naming objects on a slide every 5 seconds (commonplace objects, alternating with "AND") were initiated 2 to 5 seconds after beginning IR image acquisition (data acquisition, 36.4–60 seconds). For documentation, digital photographs were obtained before and after SSEP, and cortical stimulation tickets were placed on the cortex.

Standards for Intraoperative Cortical Localization

The standards for location of the somatosensory cortex were cortical SSEP mapping in response to contralateral median nerve stimulation (21 cases; 15 with results adequate to localize the central sulcus, 2 results adequate to identify the sensory cortex, 3 cases inadequate for cortical localization) and elicitation of sensation by cortical stimulation (16 local anesthesia cases). Motor cortex localization was by elicitation of a motor response to cortical stimulation (11 cases). Localization of language/speech cortex was by speech arrest and anomia during intraoperative cortical stimulation[9,10] using tasks identical to language tasks during IR recording (six cases). Bipolar (5mm between tips) cortical stimulation (50/second, 2–12mA) was with an electrical stimulator (Grass model 2; Grass Instruments); 4 to 8mA was necessary for a response. A 16-channel electroencephalogram recorder monitored after-discharges. If after-discharges occurred, further stimulation was delayed until they abated spontaneously or disappeared after cortical irrigation with cooled Ringer's lactate.[11] Each stimulation train was limited to 2 to 4 seconds. Motor response, speech arrest, sensations, and experiences were documented. Based on the results, tickets were placed over each stimulation site (central point between the electrode tips).

Functional Magnetic Resonance Imaging

Preoperative fMRI of 13 patients were performed during finger tapping (sensorimotor task). Four scans could not be analyzed because of noise (head motion in patients with brain tumors). Patients were asked to touch their fingers (starting with the index finger, sequentially backward and forward) to their palm, approximately one tap per second. Echo planar images were acquired using a GE 1.5T scanner with TR of 2 seconds and TE of 40 milliseconds. The boxcar design paradigm used 75 scans at rest followed by 75 scans during the task. MEDx computer software (MEDx 3.2, Sensor Systems, Sterling, VA) was used to correct for head motion (automatic image registration [AIR] 3.08), Gaussian smoothing with 10mm full-width at half-maximum, voxel-by-voxel linear detrending of the time series, and *t* test between task versus rest conditions. A *Z*-score over 4 was chosen as the threshold.[12,13] These functional maps were fused to a T1-weighted, contrast-enhanced, three-dimensional MRI data set (SPGR) using MEDx computer software. Thus, an MRI surface image of the cerebral cortex with the activated areas shown by fMRI was created.[14,15]

Temporary Occlusion of Arteries

To examine the basis of the IR signal from the brain (blood flow vs cortical metabolic activity), when cortical incision was indicated during temporal lobectomy, we occluded a small (approximately 0.5mm diameter) surface artery, the distribution of which was to normal-appearing superficial cortex within the tissue to be excised, for 1 minute with a temporary aneurysm clip. IR imaging began 30 seconds before occlusion and continued until 60 seconds after occlusion.

Data Analysis

Successive trials of IR images were acquired with at least 1 minute between trials, consisting of periods of rest (baseline) and activation (stimulation) and were stored (Axil Ultima workstation; Axil Computer, Santa Clara, CA). To analyze the data on-line (ENVI software; Research Systems, Boulder, CO), we calculated normalized difference images (pixel-by-pixel the mean baseline values were subtracted from stimulated values and divided by the mean baseline values) to define the topography of functionally induced thermal gradients. Trials with minimal motion artifact were used without signal detrending, filtering, or averaging. For visualization of an *intensity map* in the operating room, the difference image with maximal signal intensity was color-coded.

In instances of multiple images with maximal signal intensity, an image and epicenter were selected for further analysis. To minimize subjectivity, we performed Student's *t* test for each IR trial off-line to determine significant differences in pixel intensity between groups of images collected during periods of rest and activation. The test was performed for each pixel and one image, a *Z*-score parametric map, was generated for each trial (MEDx 3.2, Sensor Systems). To determine which pixels in the *Z*-map achieved statistical significance, we performed Bonferroni correction, counting all pixels in the *Z*-map in the multiple comparison correction. The corresponding *Z*-value threshold was 4.8. Thus, a single "activation" image comprising all pixels meeting the defined criteria was produced.

To preserve in a single map a statistical measure of the frequency of functional activation, we calculated a frequency distribution map (three patients, selected based on the completeness of the data set of functional tasks) for off-line IR image analysis. Normalized subtraction maps were calculated for each trial (pixel-by-pixel the mean baseline values were subtracted from stimulated values and divided by the standard deviation of baseline values). If a pixel in the subtraction map had a value greater than 2 (2 standard deviations from mean baseline value), it was considered to be active, assuming a normal distribution of baseline pixel intensities. Only the activation portion of normalized subtraction maps

were combined to produce a frequency distribution map in which the value of each pixel represents the number of times this pixel is considered active. Therefore, higher pixel values on the frequency distribution map represent the frequency of functional activation in the different cortical areas.

Two graphs were created to represent the temporal IR response for each trial (1) intensity versus time (from a region of interest considered active on the *Z*-score map), and (2) the number of active pixels versus time extracted from normalized subtraction maps.

An Automatic Image Registration software package[16] was used for motion reduction between IR images for each individual trial before *Z*-score maps, subtraction maps, or frequency distribution maps were calculated.

Validation of Cortical Localization

For each case, the following images were imported into Adobe PhotoShop 5.01 (Adobe Systems, Mountain View, CA) for off-line data analysis: (1) IR background image, (2) IR functional images (one *Z*-score parametric map for each trial of functional activation), (3) digital photograph of the cortical surface, (4) digital photograph of the tickets representing the SSEP map, (5) the intraoperative cortical stimulation map, and (6) the activated voxels on fMRI were projected on the three-dimensional representation of the exposed cortical area. These images were placed in separate layers, scaled, rotated, coregistered, and superimposed using anatomic landmarks.

The layered images were analyzed by evaluating the degree of agreement between the functional areas indicated by induction of temperature gradients (IR) and the areas identified by the standard techniques for operative cortical mapping and by fMRI. For intraoperative cortical stimulation the extent of the cortical area subserving a specific cortical function was defined by a circle (radius, 5mm) with its center at a positive stimulation site,[17] and for SSEP localization of the central sulcus was by a circle (radius, 15mm) with its center at the midpoint between electrodes showing a SSEP phase change. For fMRI, a three-dimensional representation of the exposed cortical area was displayed with the activated voxels identified at a depth of up to 3mm from the cortical surface by fMRI projected on the surface. For each case, the relationship of standard and IR localization was categorized with a three-letter scale: "A," IR focus within the area determined by standard localization, "B,"IR focus partially ($>1mm^2$) inside and partially outside the area determined by standard localization, and "C," IR focus outside the area determined by standard localization. The average category between three IR trials for each sensory and motor functional task (underlined letters in the Table) was used to compare the standards with the IR localization.

Results

Baseline Infrared Imaging with Exposed Cortex

Baseline IR images showed cortical temperature heterogeneity between 27 and 34°C (Fig 1A). The images included multiple irregular thermal compartments (warm and cool patches) and distinctive vascular patterns. Comparison of visible light and IR background images showed that the warmest sites corresponded to the superficial vasculature (see Fig 1A–C). The coolest sites were in the center of exposed gyri. Multiple small vascular elements were present between the warmest and coolest patches. Arteries appear bright (high temperature), the cortical surface appears dark gray (low temperature), and veins appear light gray (intermediate temperature). The temperature gradient between arteries and veins was 1.5 to 2.0°C and between veins and brain parenchyma was 0.2 to 1.0°C. Some showed no temperature gradients with surrounding brain and therefore were not visible on the IR image. Some small diameter vessels of high temperature (arteries) appeared to have a larger diameter on the IR image than their size at surgery on visible light photographs.

Direct IR observation of superficial cerebral arteries showed pulsatile segmental perfusion (rhythmic contraction and dilation). Less IR pulsatility was detected in the veins and almost none occurred in parenchyma (Fig 2).

Generally, the topical location of surgically verified lesions was identified by a low temperature or high temperature at the site of the lesion relative to the surrounding cortex (see Fig 1A). Although the epicenter of tumor involvement often could be distinguished from adjacent brain, temperature heterogeneity occurred within individual lesions (report in preparation).

Functional Infrared Imaging

Neural activation elicited reproducible temperature increases (0.04–0.08°C) within the primary somatosensory cortex during median nerve stimulation, in the sensorimotor cortex during repetitive hand movements and finger tapping, and in language areas during speech production (intensity map). The sites of maximum functionally induced temperature colocalized with individual segments of small vessels (mainly pial arteries and arterioles) and at parenchyma sites which did not follow the surface patterns of individual gyri (see Table).

*Fig 1. Intraoperative infrared (IR) images of the exposed cortex in a patient with a right frontal oligodendroglioma (Patient #1; frontal is left upper corner, vertex at bottom). (A) On the baseline IR gray scale image, the surface vessels, especially the arteries, appear lighter (warmer) than the surrounding cortex. The IR emission from the cortical region overlying the tumor (*arrow *in A) is lower than the surrounding cortex. (B) The functional IR pseudocolor image (intensity map) produced during contralateral median nerve stimulation identifies a discrete area of increased IR emission. (C) Intraoperative visible light photograph identifying the exposed cortical region activated by somatosensory stimulation* (arrow).

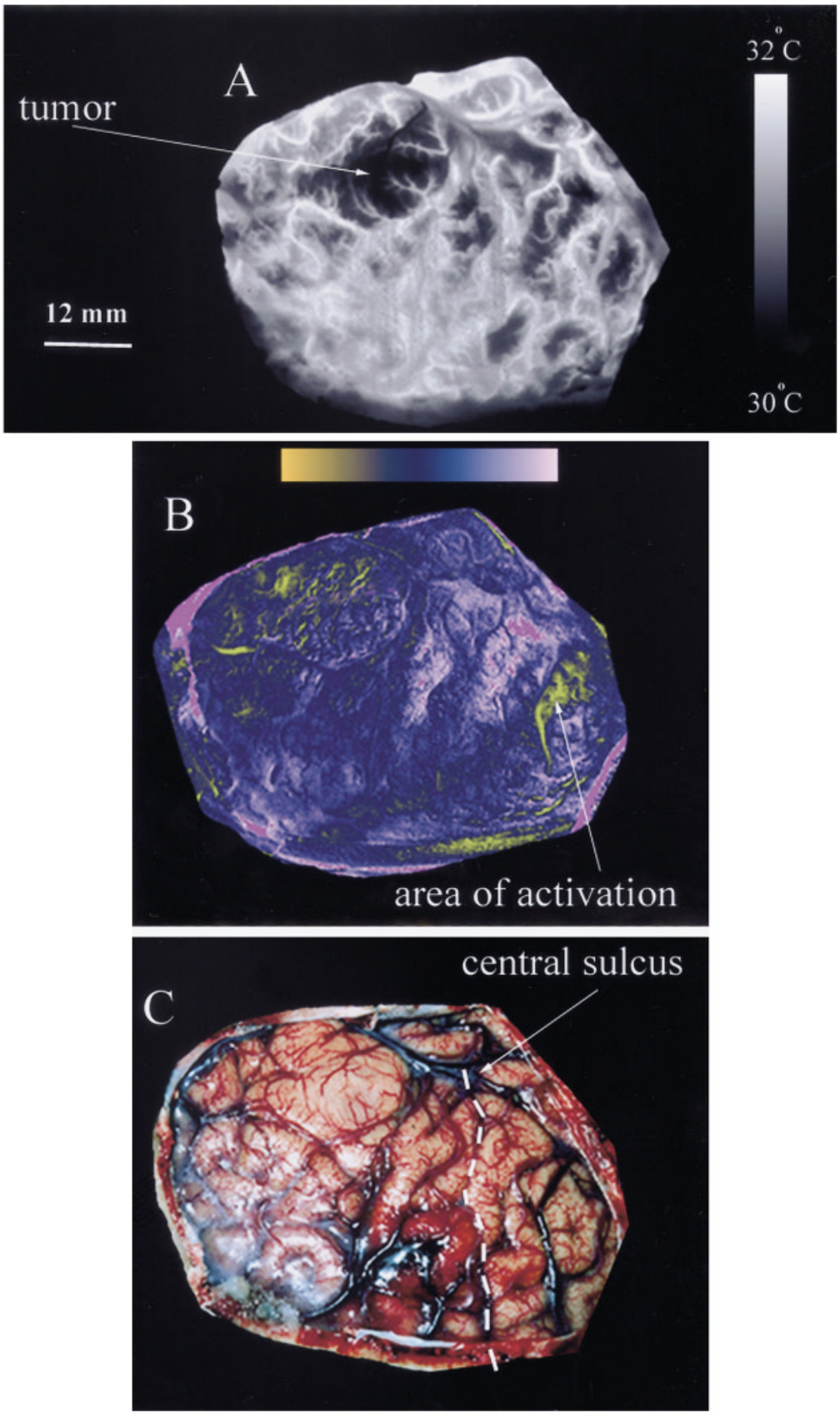

Figure 1

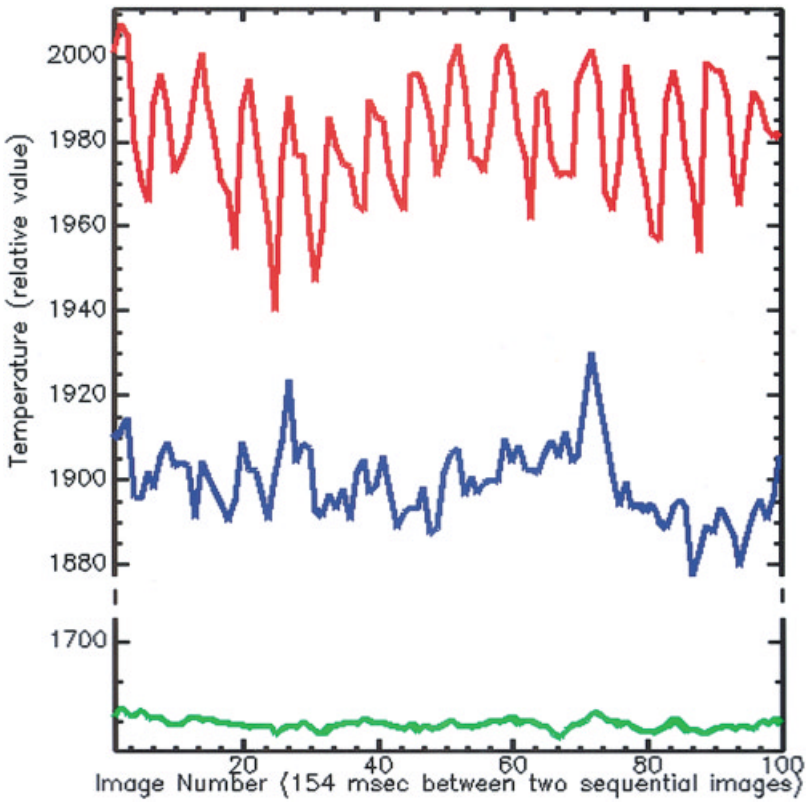

Fig 2. Temperature profiles for superficial artery (red), vein (blue), and parenchyma (green) extracted from 100 infrared (IR) images collected during 15.4 seconds of direct observation of exposed human brain. The same region-of-interest size (2 × 2 pixels) was chosen for the different vasculature and cortical sites. Note cyclic temperature alteration (pulsatile segmental perfusion of the cerebral artery) related to heartbeat and that the temperature of the vein is intermediate between the temperature of the artery and the brain surface.

Although the initial temperature responses were detected as early as 100 milliseconds, peak IR responses occurred 5 to 7 seconds after stimulus onset. The intensities of the IR responses varied with different tests, with the lowest magnitude IR responses occurring with median nerve stimulation and the highest with the repetitive motor test (ball squeezing). Only the highest intensity IR responses (exceeding the 90th percentile) were spatially confined to regions identified as functionally active by the intraoperative cortical stimulation map and the SSEP map. In most instances, lower intensity IR responses (50th to 90th percentile change in intensity from baseline) arose in the vicinity of the maximum responses and occurred frequently at sites remote from the sites of maximum response.

The shape and number of discrete sites exceeding the 90th percentile, as well as the number of activated pixels within each site, varied from image to image within a single IR trial. The intensity of the IR signal changes and the number of activated pixels in the primary motor cortex were synchronized with motor activity during sequential ball squeezing (Fig 3A). Sites in the premotor area, primary motor cortex, and primary sensory area were activated sequentially over 0.5 to 4.0 seconds during this motor task (see Fig 3B). This was clearly observed in four patients but was not observed in the other seven patients who performed this task. The most intense IR responses evoked by language tasks were restricted to the receptive (Wernicke's) and expressive (Broca's) speech areas (four of six patients), defined by intraoperative cortical stimulation mapping (Fig 4). Additional cortical areas were activated to a lesser degree (see Fig 4).

Comparison of the intensity, *Z*-score parametric, and frequency distribution maps did not show substantial differences in the spatial distribution of thermal gradients between these three methods of analysis, although for all three maps the extent of the IR activations varied with the analysis threshold chosen. To minimize subjectivity for comparison between IR and standards for cortical localizations, we chose only the *Z*-score parametric map approach, and the same p value less than 0.01 (*Z*-scores between 5 and 15) was used for all patients.

Variability in the location, number, size, and shape of activated sites was observed on *Z*-score maps among patients for the same sensory, motor, and language tests. Within subjects, the number, size, and shape of IR responses varied between single trials, but the pixels with maximum *Z*-score values were spatially colocalized to regions of activated cortex as defined using the standards. During median nerve stimulation, the most intense pixels on the *Z*-score maps for IR responses evoked were partially or fully restricted to the somatosensory and motor cortex (Fig 5) defined by intraoperative cortical stimulation mapping and SSEP map-

ping (see Fig 5) in 16 of 18 patients. Among the 18 patients in whom the sensory cortex was exposed at surgery, the sensory region detected by the established *Z*-score threshold during a sensory task was entirely (three patients, category "A" result) or partially (13 patients, category "B" result) within the positive response circle. There were two cases of discordant sensory localization ("C" result; see Table).

During motor tasks the most intense sites of activation were partially or fully located in the sensory-motor areas (Fig 5G,H). A match between intraoperative cortical stimulation and IR localization of motor areas (*Z*-score map) was achieved for the 11 cases (1 "A," 10 "B," 0 "C") in whom motor function was tested. The most intense sites of IR activation were colocalized with fMRI sites of activation in four of six patients with fMRI voxels of up to 3mm from the cortical surface (see Fig 5C). In three patients, the voxels activated on fMRI did not reach within 3mm of the surface.

With the stated threshold (*Z*-score map with $p < 0.01$) in 18 of 20 patients pronounced increases in the value of the IR-derived *Z*-score map during sensory and motor tasks occurred in the same regions identified by the standard mapping procedures (see Table).

Among the six analyzed cases in which language cortex was exposed, colocalization of language-related areas occurred in four patients (4 "B", 2 "C"). In the "C" patients, in whom no focal activation was detected with IR images, standard mapping localized Wernicke's area to a posterior portion of the left superior temporal gyrus that was discolored because of tumor infiltration and was hypovascular because of radiation injury. In two of six awake patients in whom Broca's area was exposed the motor and language tests produced enhanced temperature (*Z*-score map) in Broca's area.

Infrared Imaging During Vessel Occlusion

Temporary occlusion of a small cortical artery (four patients) immediately reduced the IR signal from the occluded vessel and from the cortical region perfused by it. The IR signal rapidly returned to normal after the occlusion was relieved.

Discussion

Basis of Infrared Imaging of the Brain

The camera used in this study is sensitive to IR photons emitted from the brain as a result of natural IR radiation. The energy of IR photons emitted from deeper brain structures is attenuated by surface tissues.

Arterial blood at core temperature is warmer than the exposed brain surface, which has been cooled by evaporation and room air.[18–20] Therefore, local microvascular CBF can be used as an endogenous, natural thermal contrast agent for IR monitoring of the brain during surgery. To characterize the contribution of CBF in the IR signal, we analyzed the convective component of heat transfer. If arterial blood is at core temperature, takes on the temperature of deeper brain regions, and carries this heat to the surface, the major factors that influence the convective distribution of heat can be estimated as:

$$Q_{CBF} \approx C \cdot \rho_B \cdot CBF \cdot \Delta T$$

where Q_{CBF} is the convective component of heat transfer, C (specific heat capacity of the blood) is 0.93cal $\cdot$ gm^{-1} $\cdot$ $degree^{-1}$, p_B (blood density) is 1gm $\cdot$ ml^{-1}, CBF is 0.8 ml $\cdot$ gm^{-1} $\cdot$ min^{-1} for human cortex gray matter,[21] and δT is the temperature gradient between the depth of the cortex and the surface. In our studies (temperature measurement on the cortical surface and within sulci using thermocoupling at surgery) and intraoperative studies by others,[19] it averaged 2.0°C . Thus, $Q_{CBF} \approx 1.49$cal $\cdot$ gm^{-1} $\cdot$ min^{-1}. If we assume temperature differences of arterial blood at a core temperature of 37°C and a surface temperature of 31°C (see below), the heat presented to the brain surface by arterial flow is even greater (≈ 4.46cal $\cdot$ gm^{-1} $\cdot$ min^{-1}).

For intact brain, the amount of metabolic heat locally generated per gram of brain is 0.16cal $\cdot$ gm^{-1} $\cdot$ min^{-1}.[22] Because the cortical temperature in this study was measured as 31°C average, the metabolic rate of the cortex and its accompanying metabolic heat production are depressed even further, enhancing the difference between the CBF-related and metabolic heat–related values. Furthermore, during functional activation local increases in the activity of neuronal assemblies induce regional variations of blood flow and blood volume, glucose utilization, and oxygen consumption. Local CBF increases by local vasodilation.[23,24] Positron emission tomography studies have shown CBF changes of 30% during somatosensory stimulation.[25] Therefore, the heat contributed by CBF is 10 to 30-fold higher than is contributed by brain metabolism. Finally, occlusion of small arteries at surgery produced an immediate and significant decrease in temperature in the artery distal to the occlusion and the tissue perfused by it, as we have described previously in animals.[20]

The sensitivity of the IR camera for temperature, space, and time demonstrated a rapid decrease in temperature during the fraction of a second occupied by diastole, during which blood flow is interrupted (see Fig 2). This clearly indicates not only that the temperature of arterial blood rapidly decreases at the cortical surface, but also indicates the delivery of blood at higher temperature during systole. The cortical veins, which reach the surface from deep brain areas, have a temperature that is higher than the superficial brain

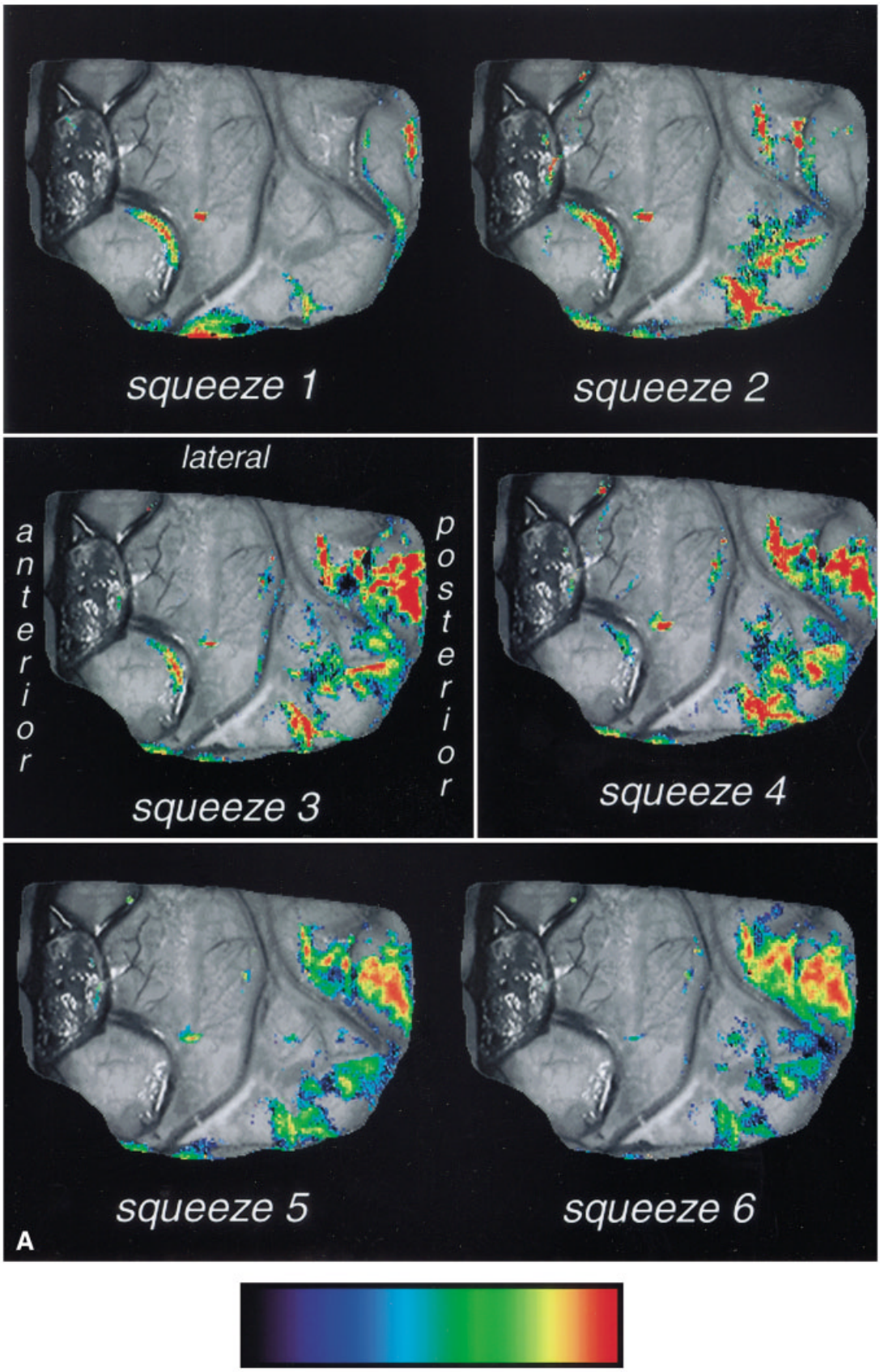

Fig 3. Figure and legend continue.

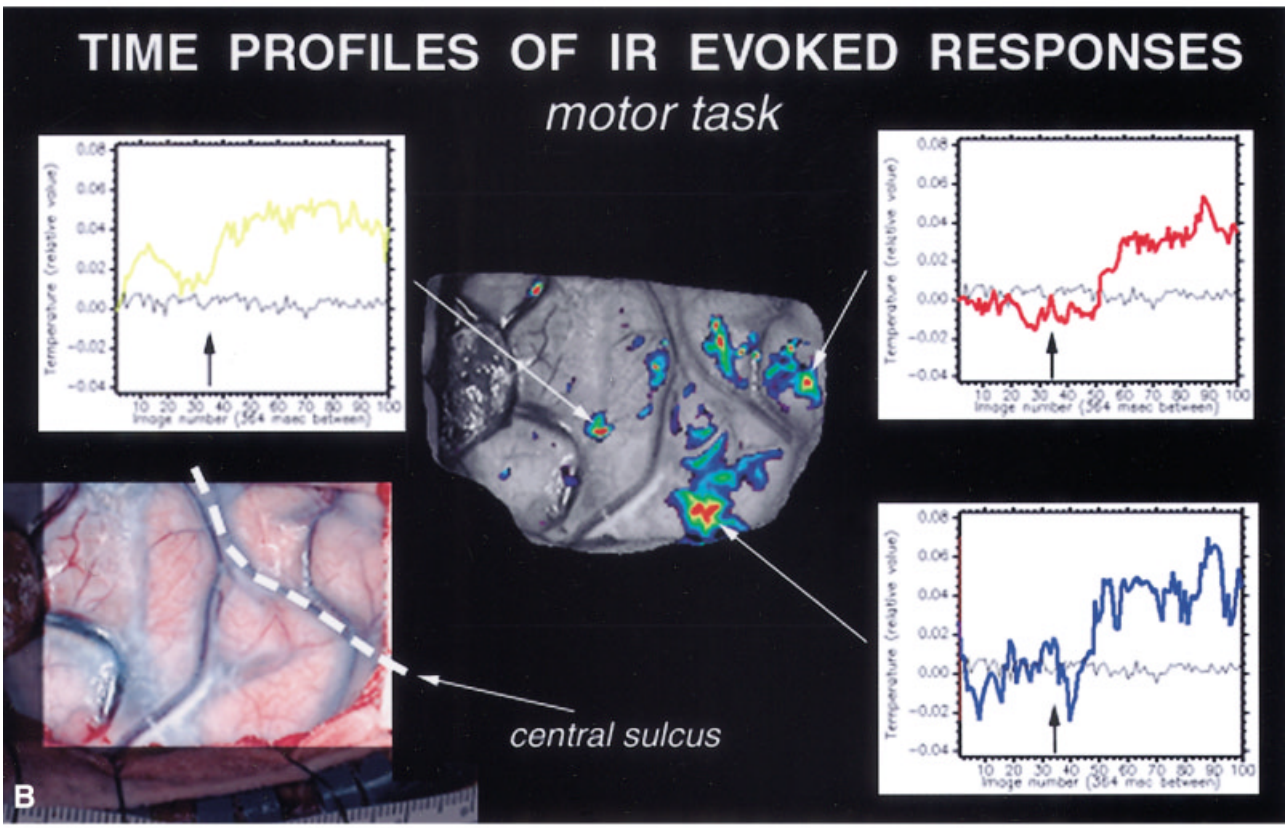

Fig 3. (continued.) (A) Functional infrared (IR) images of the brain during serially squeezing a ball in the contralateral hand (motor task). Six IR images (pseudocolored intensity map) were chosen among 100, registered, and layed over a digital image of the exposed cortex (gray). Each image represents temperature changes of the cortex during individual squeezes of the ball at 4, 10.9, 14.5, 18.9, and 22.5 seconds after the command was initiated (see B, blue graph). Note that the intensity of the IR signal and the number of activated pixels changes from squeeze to squeeze in the primary motor and sensory cortex. (B) Temporal aspect of IR responses evoked by the motor task (ball squeezing). Chosen automatically from a reconstructed Z-score map, three distinct regions of interest (each of 10–15 pixels of maximum Z-value) were transferred to a normalized difference IR images set. After that, the temperature profiles (IR intensity vs *time) were plotted from 100 normalized difference IR images collected during 36.4 seconds, 12.7 seconds of baseline, and 23.7 seconds of serially squeezing a ball in the contralateral hand (starting at image 35). Note the sequential increase of the latency period (time to the onset of temperature change) for different regions identified as premotor cortex (yellow), primary motor cortex (blue), and sensory cortex (red). Temperature profiles extracted from an area not involved with functional activation are shown on each graph (black) for comparison.*

temperature, reflecting the higher temperature of the brain at deeper levels. Because the main contributor of brain surface temperature gradients during intraoperative conditions is CBF, the detected functionally evoked IR signals are directly dependent on evoked local CBF. Thus, the local increases in cortical CBF induced by neuronal activation should be seen on IR functional images and, because local cortical capillary CBF is tightly linked in time and space to neural function,[7,8] IR functional images should map in a manner that depicts cortical activation.

The temporal analysis of IR activation showed that the vascular system responds immediately (100–1,000 milliseconds or faster) after functional stimulation, whereas the peak intensity of the IR response occurred at the same latencies as the well-described fMRI response (5–10 seconds after stimulus onset).[26,27]

Mapping of Cortical Function: Correlation of Infrared and Conventional Approaches

Sites of maximum signal on the "functional" IR maps overlapped with localization by the IR, ICS, and fMRI techniques. In every instance but four, the cortical sites showing maximum temperature change from baseline during sensory, motor, or language tasks were located in the same regions identified by SSEP and intraoperative cortical stimulation mapping. The distribution of the changes in IR signal induced by functional tasks also overlapped with the areas defined by fMRI as be-

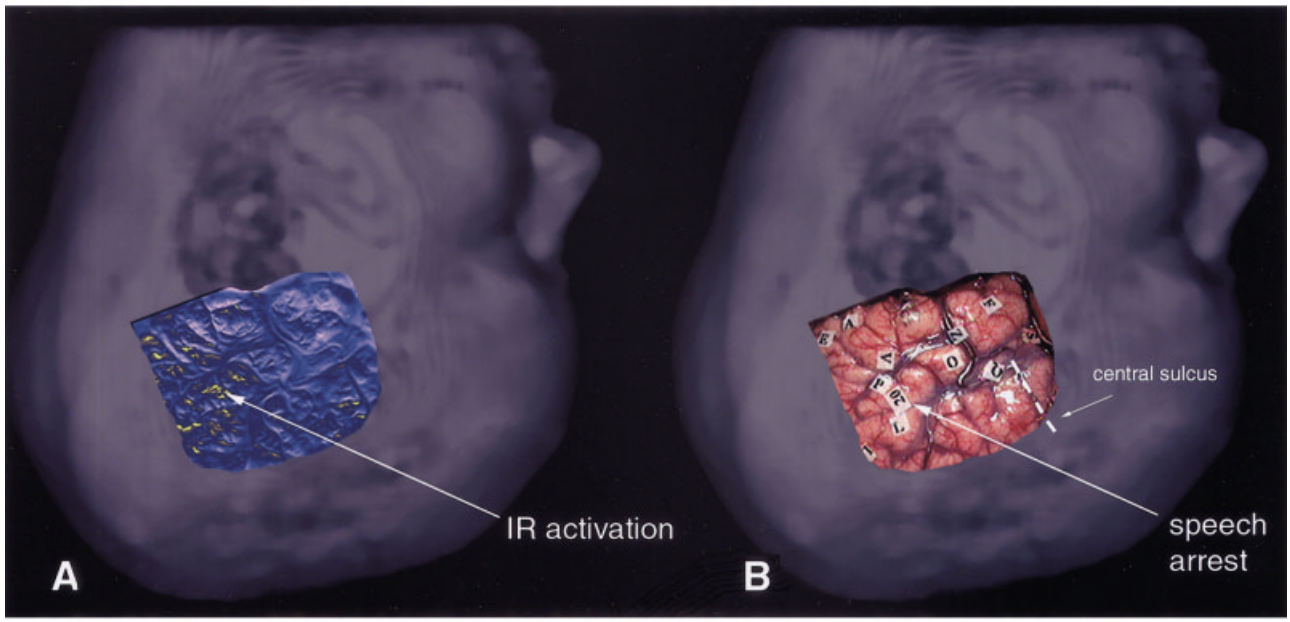

Fig 4. Functional infrared (IR) image of the brain during naming an object (verbal task). The IR image with maximum signal intensity was chosen among 100, registered, and layed over an magnetic resonance imaging–derived three-dimensional image of the patient's head (Patient 16). Note that the site of the maximum intensity of the IR signal (yellow, A) and the site where intraoperative cortical stimulation evoked speech arrest (Wernicke's area, ticket 20 on exposed cortex, B) have the same location. Note activation of additional cortical areas during naming (A).

ing activated during similar tasks. However, functional IR imaging showed several important differences.

Rapid and Continuous Imaging Is Provided

The IR method allowed us to rapidly (as rapidly as every 14 milliseconds) and continuously acquire from the exposed cerebral cortex an image of the distribution of activation in response to initiation and maintenance of a functional task or in response to median nerve stimulation. This contrasts with the comparatively prolonged interval (seconds to minutes) required to acquire each image with conventional techniques of functional imaging or functional localization.

Infrared Imaging of Brain Function

An advantage of the IR mapping approach is that it permits rapid acquisition of a continuous surface image of activation, showing the distinct shape and borders of areas of activation within the exposed cortex with high sensitivity and precision (100–350μm in this study). Thus, it allows continuous assessment of sites of activation simultaneously over a wide cortical region. In contrast, other available techniques permit only assessment of discontinuous discrete areas (1) each at a single instant (cortical stimulation), the function of the intervening cortex requiring estimation by mental interpolation, or (2) the product of an accumulation of signals over an extended interval at a single (somatosensory evoked potentials [EP]) or multiple (fMRI) sites. Differences in mapping methodology may explain the differences in the distribution of activation detected using the various approaches in this study. Furthermore, the ability to detect functional activity without averaging significantly contributes to the study of cortical dynamics.

Distribution of Function

Although the location of the IR epicenters (using the intensity maps, *Z*-score maps, and frequency distribution maps) corresponded with the functional locations demonstrated by the intraoperative cortical stimulation, somatosensory, and fMRI maps, the IR activation was more widespread than was detected with the use of the other approaches.

Analysis of the intensity, *Z*-score, and frequency distribution maps while using conservative thresholds showed the IR response to occur in a spatially confined area of high intensity, whereas analysis with less conservative thresholding showed more widely distributed areas of low-intensity activation within the somatosensory and motor cortex. The overlapping representations for sensory and motor tasks on the IR images were in contrast with the discrete regions without overlap on cortical stimulation maps (see Fig 5). The distribution detected by IR imaging may include association cortex underlying the motor imagery and movement prepara-

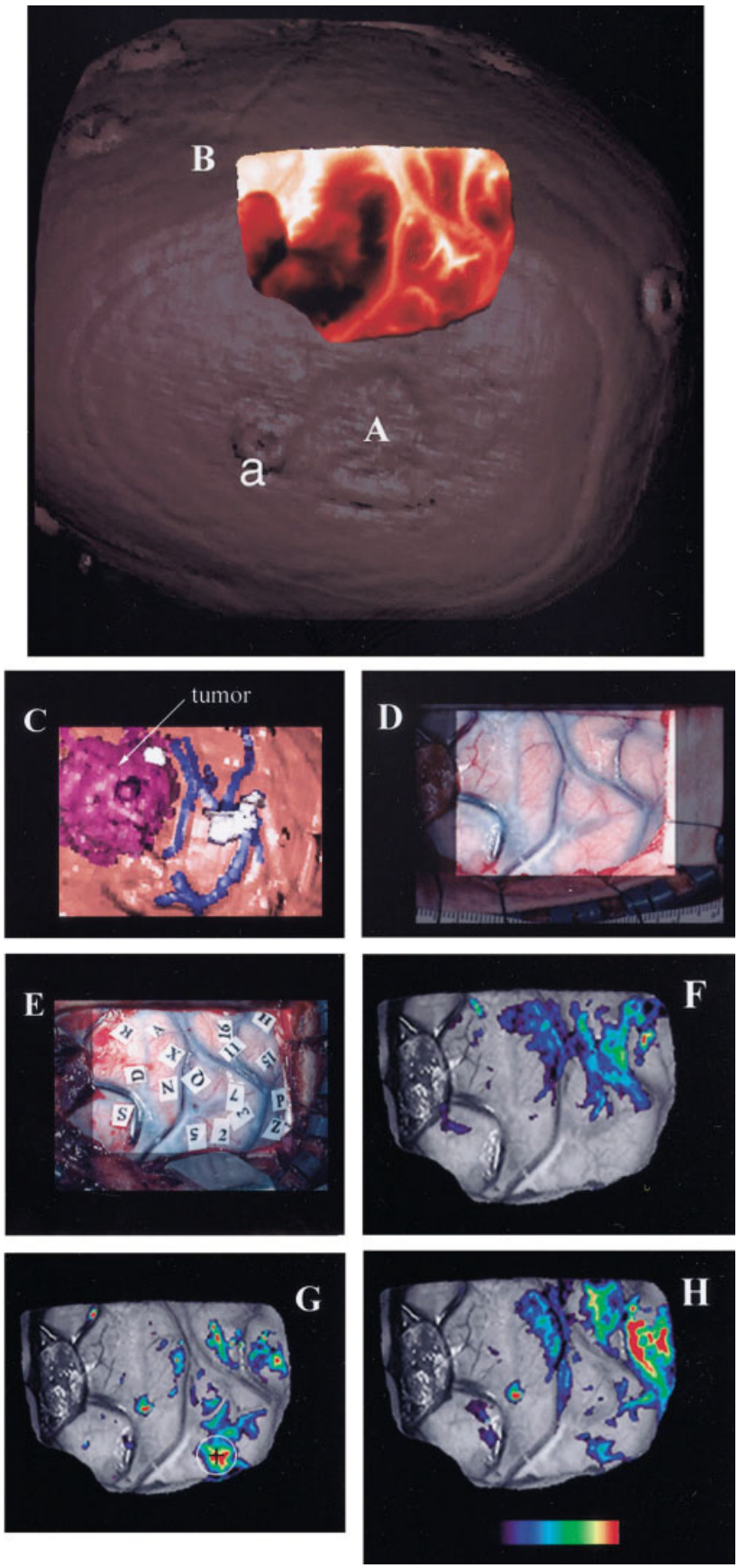

Fig 5. Comparison of infrared (IR) imaging with standard cortical mapping and functional magnetic resonance imaging (fMRI). Adenocarcinoma metastatic to the right frontal and parietal lobes (Patient 18, same patient as in Fig 3). (A) Preoperative three-dimensional MRI image of the head. (B) Background intraoperative IR image. (C) Areas activated on fMRI by finger tapping are shown in white. Three-dimensional colorized image of the tumor (purple) and surface veins (blue) obtained from contrast-enhanced MRI and displayed in the same orientation as the intraoperative images. (D) Intraoperative digital photograph of the cortex. (E) Tickets indicating the results of direct cortical stimulation: motor responses (2, 3, 5, 7, and Q), sensory responses (11, 15, and 16), no response (Z, P, H, X, N, S, D, A, and R). Functional IR responses (color sites, overlaid gray cortical photograph) were evoked by median nerve stimulation (F), hand squeezing (G), and finger tapping (H). In G, a 10mm circle has been drawn around the site where cortical stimulation evoked flexion of the contralateral hand. During finger tapping, 54% of the activated pixels on the fMRI image (C) were colocalized with activated pixels on the functional IR image (H). MRI representation of patient's head (A) with fiducial markers (a) was used as a template on which all other images were superimposed.

tion that is followed by the motor act. Similarly, analysis of the language tests using a less conservative threshold (reasonable elements corrected critical threshold[28]) showed multiple areas of activation, including areas outside the traditional sites to which language has been assigned, suggesting that additional regions are used for the complex cognitive aspects of language/speech production and that they can be detected by IR imaging.

The extent of activation on IR images by a motor performance was much larger than the area required to elicit the movement by electrical stimulation. The detailed IR-derived spatial maps of activated cortical regions during motor performance provide evidence against the hypothesis that somatosensory and motor areas contain single, discrete, topographically organized regions for motor control. Rather, the distribution observed via IR mapping was more widely spread and comprised spatially segregated, cluster-like sites that did not appear to be organized topographically around an epicenter. These findings are consistent with the recent observations of others[29] and their proposals that the activation of the cortex for motor function is more distributed and more complex[29–31] than the discrete loci demonstrated by brief cortical stimulation during surgery or by the noninvasive functional imaging techniques.

Because the distribution of activation on the IR images was more widespread than the cortical stimulation maps, it was not possible to use the IR activation maps to determine maximal safe tissue resection. Whether the IR approach can be modified to more accurately provide this function remains to be determined.

Observations via Capacity to Image a Wide Area of the Cerebral Cortex with High Resolution in Space and Time

During median nerve stimulation multiple sites of activation were limited to the somatosensory and, to lesser degree, the motor areas, without a temporal distinction of their activation. This is consistent with the hypothesis that the primary motor and sensory cortical representations of the hand overlap are functionally integrated and are not divided in a simple manner by the central sulcus.[29,31]

Sequential activation of sites in the supplementary motor area as well as in the primary motor and sensory cortex during performance of a motor task was demonstrated (see Fig 3), suggesting the existence of a functionally connected, time-coordinated cortical network within the area of activation .

Within subjects, from trial to trial and from image to image during a single trial, the shapes of the IR responses varied but did so within the limits of a selective, spatially confined region of the sensory-motor cortex. The number of activated pixels, their spatial extent, and their precise location changed (note change from squeeze 1 to squeeze 6 in Fig 3), an observation that is consistent with recruitment of new neuronal elements in the motor task. Both local vasodilation (volumetric expansion in individual vessels already perfused) and recruitment phenomenon (changes in the proportion of vessels perfused during different stages of functional activation) may be reflected in these series of images. Such plastic changes (moment by moment local readjustment to changing functional demands) do not have the potential to be observed using other approaches for detecting brain function in humans.

By providing information on the spatial and temporal patterns, anatomical extent, and spatial constraints of altered sensory-motor representation, IR imaging may prove to be a useful approach to study brain function.

References

1. Berger H. Untersuchungen uber die Temperatur des Gehirns. Jena: Fisher, 1910:130.
2. Baker MA, Frye FM, Millet VE. Origin of temperature changes evoked in the brain by sensory stimulation. Exp Neurol 1973; 38:502–519.
3. Salcman M, Moriyama E, Elsner HJ, et al. Cerebral blood flow and the thermal properties of the brain: a preliminary analysis. J Neurosurg 1989;70:592–598.
4. LaManna JC, McCracken KA, Patil M, Prohaska OJ. Stimulus-activated changes in brain tissue temperature in the anesthetized rat. Metab Brain Dis 1989;4:225–237.
5. Shevelev IA, Tsicalov EN, Budko KP, et al. Dynamic infrared functional mapping of the cerebral cortex. Biomed Sci 1990;1: 571–577.
6. Gorbach AM. Infrared imaging of brain function. Adv Exp Med Biol 1993;333:95–123.
7. Frostig RD, Lieke EE, Ts'o DY, Grinvald A. Cortical functional architecture and local coupling between neuronal activity and the microcirculation revealed by in vivo high-resolution optical imaging of intrinsic signals. Proc Natl Acad Sci USA 1990; 87:6082–6086.
8. Malonek D, Dirnagl U, Lindauer U, et al. Vascular imprints of neuronal activity: relationships between the dynamics of cortical blood flow, oxygenation, and volume changes following sensory stimulation. Proc Natl Acad Sci USA 1997;94:14826–14831.
9. Fedio P, Van Buren JM. Memory and perceptual deficits during electrical stimulation in the left and right thalamus and parietal subcortex. Brain Lang 1975;2:78–100.
10. Ojemann G, Ojemann J, Lettich E, Berger M. Cortical language localization in left, dominant hemisphere. An electrical stimulation mapping investigation in 117 patients. J Neurosurg 1989;71:316–326.
11. Sartorius CJ, Berger MS. Rapid termination of intraoperative stimulation-evoked seizures with application of cold Ringer's lactate to the cortex. Technical note. J Neurosurg 1998;88: 349–351.
12. Yousry TA, Schmid UD, Jassoy AG, et al. Topography of the cortical motor hand area: prospective study with functional MR imaging and direct motor mapping at surgery. Radiology 1995; 195:23–29.
13. FitzGerald DB, Cosgrove GR, Ronner S, et al. Location of language in the cortex: a comparison between functional MR imaging and electrocortical stimulation. AJNR Am J Neuroradiol 1997;18:1529–1539.

14. McDonald JD, Chong BW, Lewine JD, et al. Integration of preoperative and intraoperative functional brain mapping in a frameless stereotactic environment for lesions near eloquent cortex. Technical note. J Neurosurg 1999;90:591–598.
15. Yetkin FZ, Mueller WM, Morris GL, et al. Functional MR activation correlated with intraoperative cortical mapping. AJNR Am J Neuroradiol 1997;18:1311–1315.
16. Woods RP, Grafton ST, Holmes CJ, et al. Automated image registration. I. General methods and intrasubject, intramodality validation. J Comput Assist Tomogr 1998;22:139–152.
17. Roux FE, Boulanouar K, Ranjeva JP, et al. Cortical intraoperative stimulation in brain tumors as a tool to evaluate spatial data from motor functional MRI. Invest Radiol 1999;34: 225–229.
18. Mellergard P. Intracerebral temperature in neurosurgical patients: intracerebral temperature gradients and relationships to consciousness level. Surg Neurol 1995;43:91–95.
19. Stone JG, Goodman RR, Baker KZ, et al. Direct intraoperative measurement of human brain temperature. Neurosurgery 1997; 41:20–24.
20. Watson JC, Gorbach AM, Pluta RM, et al. Real-time detection of vascular occlusion and reperfusion of the brain during surgery by using infrared imaging. J Neurosurg 2002;96:918–923.
21. Siesjo. Brain energy metabolism. New York: Wiley, 1978.
22. Yablonskiy DA, Ackerman JJ, Raichle ME. Coupling between changes in human brain temperature and oxidative metabolism during prolonged visual stimulation. Proc Natl Acad Sci USA 2000;97:7603–7608.
23. Ngai AC, Meno JR, Winn HR. Simultaneous measurements of pial arteriolar diameter and laser-Doppler flow during somatosensory stimulation. J Cereb Blood Flow Metab 1995;15: 124–127.
24. Rovainen CM, Woolsey TA, Blocher NC, et al. Blood flow in single surface arterioles and venules on the mouse somatosensory cortex measured with videomicroscopy, fluorescent dextrans, nonoccluding fluorescent beads, and computer-assisted image analysis. J Cereb Blood Flow Metab 1993;13:359–371.
25. Seitz RJ, Roland PE. Vibratory stimulation increases and decreases the regional cerebral blood flow and oxidative metabolism: a positron emission tomography (PET) study. Acta Neurol Scand 1992;86:60–67.
26. Turner R. fMRI: methodology–sensorimotor function mapping. Adv Neurol 2000;83:213–220.
27. Ogawa S, Lee TM, Kay AR, Tank DW. Brain magnetic resonance imaging with contrast dependent on blood oxygenation. Proc Natl Acad Sci USA 1990;87:9868–9872.
28. Worsley KJ, Evans AC, Marrett S, Neelin P. A three-dimensional statistical analysis for CBF activation studies in human brain. J Cereb Blood Flow Metab 1992;12:900–918.
29. Toni I, Shah NJ, Fink GR, et al. Multiple movement representations in the human brain: an event-related fMRI study. J Cogn Neurosci 2002;14:769–784.
30. Graziano MS, Taylor CS, Moore T. Complex movements evoked by microstimulation of precentral cortex. Neuron 2002; 34:841–851.
31. Schieber MH. Constraints on somatotopic organization in the primary motor cortex. J Neurophysiol 2001;86:2125–2143.